JOURNAL OF AIRCRAFT
Vol. 34, No. 3, May–June 1997

Engineering Notes

ENGINEERING NOTES are short manuscripts describing new developments or important results of a preliminary nature. These Notes cannot exceed 6 manuscript pages and 3 figures; a page of text may be substituted for a figure and vice versa. After informal review by the editors, they may be published within a few months of the date of receipt. Style requirements are the same as for regular contributions (see inside back cover).

Derivation of Four-Digit Airfoils from the Sunya Airfoil

P. Ramamoorthy*
National Aerospace Laboratories,
Bangalore 560 017, India

Introduction

RECENTLY[1,2] the author gave the properties of two new airfoils, called Sunya and Osho, which he obtained as a consequence of an analytical airfoil representation given by him earlier.[3] A class of four-digit airfoils are obtained using the Sunya airfoil and these are called the National Aerospace Laboratories (NAL)-00XX airfoils where the last two digits give the thickness in percentage of the chord. Four-digit NACA-00XX airfoils are also compared with the present airfoils. It is concluded that the Sunya airfoil, described by a simple analytical expression, could possibly be considered as a standard for all single parameter airfoils.

Content

Since the Sunya airfoil appeared[1,2] it was conjectured that NACA four-digit airfoils, which are also single parameter airfoils with a blunt trailing edge, may be derived from it. In terms of the maximum thickness ratio the NACA-00XX and Sunya airfoils can be expressed as

$$Y_{\text{naca}} = 5t_{\max}(0.2969\sqrt{X} - 0.126X - 0.3516X^2 + 0.2843X^3 - 0.1015X^4) \quad (1)$$

$$Y_{\text{sunya}} = kt_{\max}(2\sin^{-1}\sqrt{X} + 2\sqrt{X}\sqrt{1-X} - \pi X) \quad (2)$$

where k is a constant given by

$$k = \frac{1}{4\tan^{-1}(2/\pi)} = 0.440986$$

Table 1 gives the coordinates of 15% Sunya and NACA airfoils. Incidentally, exact incompressible nonviscous velocity distributions exist for these two airfoils. For zero incidence these are given by the following expressions:

$$\left(\frac{V}{V_0}\right)_{\text{sunya}} = \frac{1 + 2kt_{\max}\{1 - \frac{1}{2}\log[X/(1-X)]\}}{\sqrt{1 + 4k^2\{\sqrt{[(1-X)/X]} - (\pi/2)\}^2}} \quad (3)$$

$$\left(\frac{V}{V_0}\right)_{\text{naca}} = \frac{(1+A)}{\sqrt{1 + (B^2/4)}} \quad (4)$$

where

$$A = \frac{1}{\pi}\left[\frac{a_0}{2\sqrt{X}}\log\left(\frac{1+\sqrt{X}}{1-\sqrt{X}}\right) - a_1\log\left(\frac{1-X}{X}\right) - 2a_2\left[1 + X\log\left(\frac{1-X}{X}\right)\right] - 3a_3\left[\frac{1}{2} + X + X^2\log\left(\frac{1-X}{X}\right)\right] - 4a_4\left[\frac{1}{3} + \frac{X}{2} + X^2 + X^3\log\left(\frac{1-X}{X}\right)\right]\right]$$

$$B = \left(\frac{a_0}{\sqrt{X}} + 2a_1 + 4a_2X + 6a_3X^2 + 8a_4X^3\right)$$

$$a_0 = 1.4845, \quad a_1 = -0.63, \quad a_2 = -1.758$$
$$a_3 = 1.4215, \quad a_4 = -0.5075$$

Table 1 also shows the velocity distributions of these two airfoils. One can observe that the Sunya and NACA airfoils behave similarly except for a little discrepancy at the leading and trailing edges. It can be easily shown that the leading-edge radii, given by $\rho_{\text{sunya}} = 1.15558t_{\max}^2$ and $\rho_{\text{naca}} = 1.1019t_{\max}^2$, do not match.

NAL-00XX Airfoils

It was then decided to see whether there exists a class of new four-digit airfoils that can be derived, to any order of accuracy, from the Sunya airfoil. The Sunya airfoil can be equated to the NACA-00XX-like airfoil with an approximation as follows:

$$kt_{\max}(2\sin^{-1}\sqrt{X} + 2\sqrt{X}\sqrt{1-X} - \pi X) = A_0(\sqrt{X} + b_1X + b_2X^2 + b_3X^3 + b_4X^4 + \cdots) \quad (5)$$

where A_0, b_1, b_2, etc., are the constants to be determined.

Since the leading-edge radius of these two airfoils is required to be the same, the $\sqrt{X}$ term on the right-hand side is brought to the left-hand side. Substituting $x = \sin^2(\theta/2)$ (see Fig. 1), Eq. (5), on rearranging, becomes

$$\tfrac{1}{4}[\theta + \sin\theta - \pi\sin^2(\theta/2) - 4\sin(\theta/2)] = d_0 + d_1\cos\theta + d_2\cos 2\theta + d_3\cos 3\theta + d_4\cos 4\theta + \cdots + d_n\cos n\theta + \cdots \quad (6)$$

The fourier coefficients d_0, d_1, ... can be obtained in the usual way as

$$d_0 = -1.5$$

$$d_1 = \frac{2}{\pi}\left[-\frac{1}{2} + \frac{\pi^2}{16} + \frac{2}{3}\right] \quad (7)$$

$$d_n = \frac{2}{\pi}\left[\frac{(-1)^n - 1}{4n^2} + \frac{(-1)^{n+1} - 1}{4(n^2-1)} + \frac{2}{4n^2-1}\right]$$

Received Oct. 1, 1996; revision received Jan. 7, 1997; accepted for publication Jan. 15, 1997.

*Scientist, Computational and Theoretical Fluid Dynamics Division.

Table 1 Coordinates and the velocity distributions of NACA-0015, NAL-0015, and Sunya-15 airfoils

X	Y_{nal}	Y_{sunya}	Y_{naca}	$(V/V_O)_{nal}$	$(V/V_O)_{sunya}$	$(V/V_O)_{naca}$
0.00000	0.00000	0.00000	0.00000	0.00000	0.00000	0.00000
0.00099	0.00810	0.00810	0.00690	0.38654	0.38547	0.38380
0.00394	0.01576	0.01578	0.01361	0.70024	0.69924	0.68580
0.00886	0.02299	0.02302	0.02010	0.92875	0.92843	0.89298
0.01571	0.02976	0.02981	0.02636	1.07638	1.07689	1.02410
0.02447	0.03608	0.03614	0.03237	1.16454	1.16562	1.10530
0.03511	0.04193	0.04199	0.03809	1.21437	1.21567	1.15593
0.04759	0.04731	0.04737	0.04350	1.24084	1.24206	1.18788
0.06185	0.05221	0.05226	0.04857	1.25327	1.25423	1.20809
0.07784	0.05663	0.05667	0.05327	1.25723	1.25785	1.22059
0.09549	0.06057	0.06060	0.05756	1.25602	1.25630	1.22778
0.11474	0.06402	0.06404	0.06142	1.25161	1.25160	1.23114
0.13552	0.06699	0.06699	0.06483	1.24521	1.24498	1.23160
0.15773	0.06948	0.06947	0.06776	1.23757	1.23719	1.22978
0.18129	0.07149	0.07148	0.07020	1.22915	1.22872	1.22613
0.20611	0.07303	0.07303	0.07214	1.22027	1.21986	1.22098
0.23209	0.07412	0.07412	0.07358	1.21111	1.21079	1.21459
0.25912	0.07476	0.07477	0.07452	1.20182	1.20163	1.20718
0.28711	0.07498	0.07500	0.07498	1.19248	1.19245	1.19894
0.31594	0.07478	0.07482	0.07495	1.18315	1.18329	1.19004
0.34549	0.07419	0.07424	0.07447	1.17387	1.17417	1.18063
0.37566	0.07322	0.07329	0.07355	1.16465	1.16509	1.17083
0.40631	0.07191	0.07198	0.07224	1.15553	1.15606	1.16077
0.43733	0.07026	0.07034	0.07054	1.14648	1.14705	1.15053
0.46860	0.06831	0.06839	0.06851	1.13750	1.13807	1.14021
0.50000	0.06608	0.06615	0.06618	1.12857	1.12908	1.12987
0.53140	0.06359	0.06365	0.06357	1.11967	1.12007	1.11955
0.56267	0.06087	0.06092	0.06073	1.11076	1.11102	1.10929
0.59369	0.05795	0.05797	0.05769	1.10180	1.10189	1.09909
0.62434	0.05484	0.05485	0.05448	1.09276	1.09266	1.08896
0.65451	0.05159	0.05158	0.05115	1.08357	1.08330	1.07887
0.68406	0.04821	0.04819	0.04771	1.07418	1.07376	1.06879
0.71289	0.04473	0.04471	0.04422	1.06454	1.06401	1.05868
0.74088	0.04119	0.04116	0.04068	1.05456	1.05399	1.04848
0.76791	0.03761	0.03758	0.03715	1.04420	1.04367	1.03811
0.79389	0.03402	0.03400	0.03363	1.03336	1.03296	1.02750
0.81871	0.03045	0.03045	0.03017	1.02197	1.02180	1.01656
0.84227	0.02694	0.02697	0.02679	1.00994	1.01010	1.00517
0.86448	0.02352	0.02357	0.02351	0.99716	0.99774	0.99324
0.88526	0.02022	0.02029	0.02037	0.98351	0.98459	0.98062
0.90451	0.01707	0.01716	0.01739	0.96885	0.97048	0.96715
0.92216	0.01410	0.01421	0.01460	0.95298	0.95517	0.95263
0.93815	0.01135	0.01147	0.01202	0.93565	0.93835	0.93682
0.95241	0.00884	0.00896	0.00968	0.91650	0.91959	0.91936
0.96489	0.00661	0.00671	0.00760	0.89501	0.89827	0.89974
0.97553	0.00467	0.00475	0.00580	0.87033	0.87339	0.87716
0.98429	0.00305	0.00309	0.00430	0.84103	0.84333	0.85030
0.99114	0.00177	0.00177	0.00312	0.80438	0.80502	0.81661
0.99606	0.00085	0.00080	0.00226	0.75416	0.75156	0.77032
0.99901	0.00029	0.00020	0.00175	0.67034	0.66097	0.69287
1.00000	0.00010	0.00000	0.00158	0.00000	0.00000	0.00000

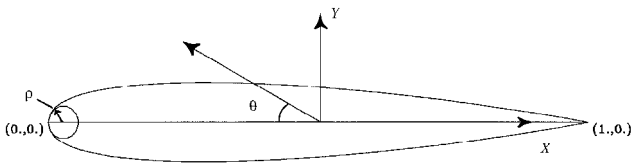

Fig. 1 Airfoil geometry.

For $n = 5$, $d_5 = 0.00013$ and as such all of the terms beyond d_4 can be neglected. With these values of d, Eq. (6) simplifies to

$$Y_{nal} = 4kt_{max}(\sqrt{X} - 0.813692X - 0.282942X^2 + 0.226354X^3 - 0.129345X^4) \tag{8}$$

Its velocity distribution is

$$\left(\frac{V}{V_0}\right)_{nal} = \frac{1 + C}{\sqrt{1 + (D^2/4)}} \tag{9}$$

where

$$C = \frac{1}{\pi}\left\{\frac{c_0}{2\sqrt{X}}\log\left(\frac{1+\sqrt{X}}{1-\sqrt{X}}\right) - c_1\log\left(\frac{1-X}{X}\right) - 2c_2\left[1 + X\log\left(\frac{1-X}{X}\right)\right] - 3c_3\left[\frac{1}{2} + X + X^2\log\left(\frac{1-X}{X}\right)\right] - 4c_4\left[\frac{1}{3} + \frac{X}{2} + X^2 + X^3\log\left(\frac{1-X}{X}\right)\right]\right\} \tag{10}$$

$$D = [(c_0/\sqrt{X}) + 2c_1 + 4c_2X + 6c_3X^2 + 8c_4X^3]$$

$$c_0 = 1.76394, \quad c_1 = -1.435336, \quad c_2 = 0.4991, \quad c_3 = 0.39928, \quad c_4 = -0.228162 \tag{11}$$

This airfoil, defined by Eq. (8), is named NAL-00XX. Table 1 also shows the coordinates and the velocity of NAL-0015 airfoil defined by Eq. (8). One can see that the NAL-0015 airfoil is similar to the Sunya airfoil of the same thickness and can provide a benchmark for analysis and testing like the NACA 0015 airfoil.

Conclusions

Since NAL-00XX airfoils are essentially equivalent to the Sunya airfoil of the same thickness there is no point in using the approximation given by Eq. (8), and as such the Sunya airfoil can be taken as a standard model for analysis and testing. NAL-00XX airfoils have only an academic interest.

References

[1]Ramamoorthy, P., "Sunya and Osho Airfoils," National Aerospace Labs., PDCF 9517, Bangalore, India, Aug. 1995.

[2]Ramamoorthy, P., "Aerodynamic Performance of Sunya and Osho Airfoils," *Current Science*, Vol. 71, No. 3, 1996, pp. 220–223.

[3]Ramamoorthy, P., and Sheela, B. V., "Airfoil Design by Optimisation," *Proceedings of the National Systems Conference*, PSG College of Technology, India, 1977.

Partial-Span Leading-Edge Vortex Characteristics in High-Rate Oscillations in Pitch

Lars E. Ericsson*
Mt. View, California 94040

Introduction

In recent pitch–oscillation tests[1] with a sharp-edged 45-deg delta wing the overall objective was to alter the development of the leading-edge vortex and decrease the extent of stall on the wing. The experimental results are of considerable interest. The modest leading-edge sweep is typical of many agile aircraft operating at high angles of attack. It produces a partial-span leading-edge vortex (Fig. 1a), such as has been observed on a wing with a 49.4-deg swept leading edge[2] (Fig. 1b).

Analysis

The time-lagged dynamically equivalent steady (DES) flow concept described in Ref. 3 is used in an attempt to define the unsteady flow physics causing the measured dramatic effects of pitching frequency on the vortex characteristics of a 45-deg delta wing[1] (Fig. 2). The flow visualization results are for the chordwise section at 45% span. Comparing the stationary results in Fig. 1a with the static data in Fig. 1b, one finds that in both cases the partial-span leading-edge vortex is located aft of or near midchord at 45% span. Judging by the measured static camber effect on the spanwise location of the leading-edge vortex[4] and, in particular, on the chordwise location of vortex breakdown,[5] one can expect the dynamic camber effect (Fig. 3) to be large for the partial-span vortex on the 45-deg delta wing.[1] The experimental results[1] for $\bar{\omega} = 2k = \omega c/U_\infty = \pi$ in Fig. 2 show that the partial leading-edge vortex stayed

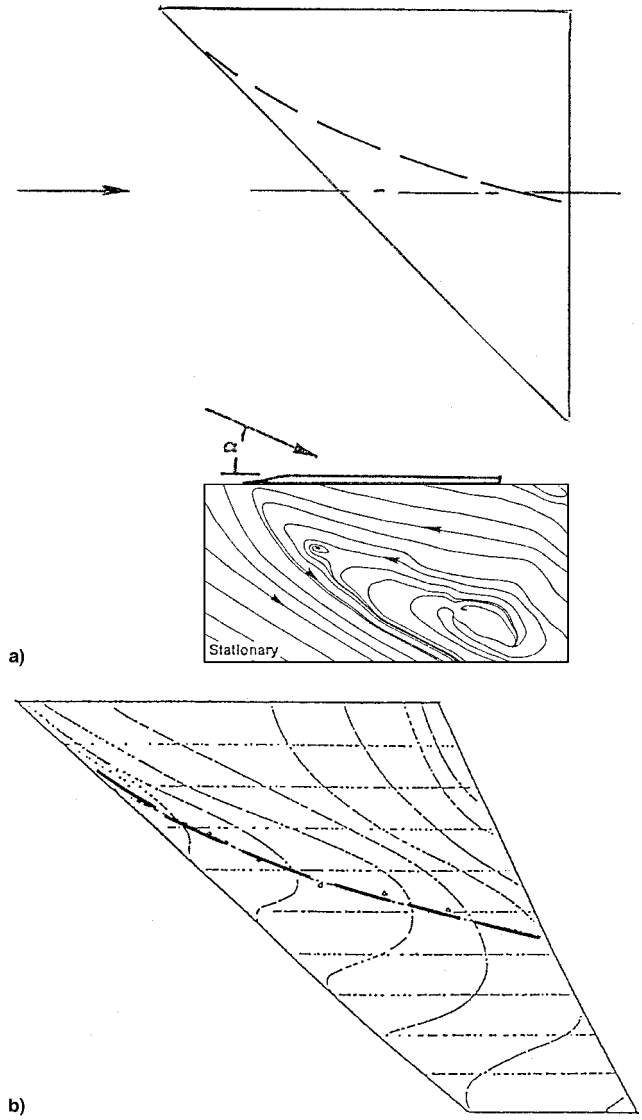

Fig. 1 Partial-span leading-edge vortices: a) 45-deg delta wing at α = 30 deg[1] and b) 49.4-deg cropped arrowhead wing at α = 20 deg.[2]

forward of the static location throughout the pitch–oscillation cycle. One expects the favorable effect of the pitch-rate-induced camber on the partial-span vortex to be analogous to that on vortex breakdown observed in pitch–oscillation tests with a 70-deg delta wing, where the vortex breakdown stayed aft of the static location throughout most of the oscillation cycle[6,7] (Fig. 4) and the extent of flow separation through vortex burst was decreased from its static value. This result is similar to the camber effect on the 45-deg delta wing, in that the extent of the lost vortex-induced lift at the leading edge was decreased. The vortex in Fig. 2 and the vortex breakdown in Fig. 4 have difficulty getting back to the stationary location because of the long transients, causing the initial static flow conditions to have a dominant effect on the dynamic characteristics.[8] If the oscillations in Fig. 2 had been initiated at C rather than A, one would expect the vortex to stay behind its stationary location throughout the oscillation cycle.

The separation-delaying action of the dynamic camber effect dominates over the α effect, causing the partial-span vortex to be located farther forward than in the static case throughout the pitch–oscillation cycle (Fig. 2). For this high frequency ($\bar{\omega} = \pi$) the favorable dynamic camber effect has already had a significant effect on the flow topology when point A is reached, resulting in a strong vortex near the leading edge.

Presented as Paper 97-0327 at the AIAA 35th Aerospace Sciences Meeting, Reno, NV, Jan. 6–9, 1997; received Jan. 15, 1997; revision received Feb. 4, 1997; accepted for publication Feb. 7, 1997.

*Engineering Consultant. Fellow AIAA.